Biomedical Microdevices 7:2, 147–152, 2005

Microfluidic Genetic Analysis with an Integrated a-Si:H Detector

T. Kamei,[*,†] *N.M. Toriello,*[**] *E.T. Lagally,*[**] *R.G. Blazej,*[**] *J.R. Scherer, R.A. Street,*[‡] *and R.A. Mathies*
Department of Chemistry, University of California, Berkeley, CA 94720, USA
E-mail: toshi-kamei@aist.go.jp

Abstract. **We have developed an integrated hydrogenated amorphous silicon (a-Si:H) fluorescence detector for microfluidic genetic analysis. It consists of a half-ball lens, a ZnS/YF_3 multilayer optical interference filter with a pinhole, and an annular a-Si:H PIN photodiode allowing the laser excitation to pass up through the central aperture in the photodiode and the filter. Microfluidic separations of multiplex PCR products generated from methicillin-resistant/sensitive *Staphylococcus aureus* (MRSA/MSSA) DNA on microfluidic capillary electrophoresis (CE) devices are successfully detected with the integrated detector. Similarly, multiplex PCR amplicons from the kanamycin resistant and K12 serotype-specific genes of *E. coli* cells are detected. The direct detection of multiplex PCR amplicons indicates that the fluorescence detector can be successfully coupled with current microfluidic PCR-CE platforms. This work establishes that the integrated a-Si:H detector provides relevant limits of detection for point-of-care genetic and pathogen analysis with microfluidic devices.**

Key Words. **integrated detector, pathogen detection, PCR, capillary electrophoresis (CE)**

1. Introduction

High resolution microfluidic capillary electrophoresis (CE) devices have been developed utilizing semiconductor industry microfabrication techniques. The precise electrokinetic manipulation of minute quantities (pL-nL) of sample in photolithographically patterned microchannels dramatically reduces analysis times. In particular, microfluidic CE based DNA restriction fragment digests (Woolley et al., 1994) and sequencing (Woolley et al., 1995) have demonstrated unprecedented high speed analysis, leading to the widespread use of microfluidic CE in various applications. Furthermore, microfabrication technology has facilitated the production of high-throughput 96 and 384-channel microfluidic CE devices for highly multiplexed genetic analysis (Emrich et al., 2002; Paegel et al., 2002).

The emphasis of lab-on-a-chip technologies is now shifting toward developing a higher degree of automation by integrating a series of analysis steps and analytical components in a single microfluidic device. For example, genetic assays may be conducted sequentially on a chip by integrating the processes of cell capture, cell lysis, DNA extraction, DNA amplification (polymerase chain reaction or PCR), purification, separation and fluorescence detection. Many microfluidic sample preparation process technologies have already been developed, including on-chip cell lysis (McClain et al., 2003), nanoliter PCR reactors coupled with high-speed CE (Woolley et al., 1996; Lagally et al., 2000), portable genetic detection of pathogens (Lagally et al., 2004) and nanoliter volume purification of DNA sequencing products (Paegel et al., 2002). However, progress is still needed in improving the performance of these biochemical components as well as in coupling these technologies. Miniaturization and integration of the fluorescence detection system is one of the most critical needs to reduce the size of lab-on-a-chip devices.

High-sensitivity microfluidic analysis typically requires fluorescence detection systems comprised of large lasers, optical systems, and detectors arranged on an optical bench, though work on miniaturized and integrated fluorescence detection systems has been reported. In one effort, a micro-avalanche Si photodiode (μAPD) was embedded in a PDMS microfluidic device and used to detect separations of proteins and small molecules (Chabinyc et al., 2001). A miniaturized spectrometer was developed using a micromachined grating and CMOS imager (Yee et al., 1997). A microfluidic system has also been integrated by depositing parylene-C over a c-Si photodiode (Webster et al., 2001). While this progress toward a miniaturized and integrated detection system is valuable, the typical c-Si photodiode fabrication method requires high process temperatures ($\sim$1000°C), rendering it difficult to directly integrate with glass- or plastic-based microfluidics.

As an alternative, we have recently developed an integrated hydrogenated amorphous silicon (a-Si:H) PIN photodiode detector consisting of *p*-type, intrinsic and *n*-type semiconductor layer (Kamei et al., 2003). The a-Si:H photodiode benefits from low deposition temperatures ($\sim$200°C) by plasma-enhanced chemical vapor deposition (PECVD) as well as *in situ* impurity doping by adding impurity gases such as B_2H_6 and PH_3 into the SiH_4

*Corresponding author.
†On leave from National Institute of Advanced Industrial Science and Technology (AIST), Tsukuba, Ibaraki, 305-8568, Japan.
**UC Berkeley/UC San Francisco Joint Bioengineering Graduate Group.
‡Palo Alto Research Center, Palo Alto, CA 94394, USA.

source gas during growth. These attributes permit the direct fabrication of an a-Si:H photodiode on inexpensive glass and plastic substrates. Additionally, the absorption coefficient of a-Si:H films is 10-fold higher than that of c-Si in the emission wavelength region (500–650 nm) of commonly used fluorophores such as DNA intercalators (e.g., thiazole orange (TO) and oxyazole yellow (YO)), fluorescein, green fluorescence protein and ethidium bromide. Furthermore, the dark current of 1 μm thick PIN a-Si:H photodiode ($\sim$100 fA/mm^2 under a reverse bias of 1 V, 25°C) is much lower than that of c-Si, facilitating low-noise detection. For these reasons, an a-Si:H photodiode is advantageous for the fabrication and operation of integrated detectors for microfluidic devices.

Here, we report the development of an a-Si:H PIN fluorescence detection module for PCR amplicon separations performed in glass CE microdevices. The integrated detection system is comprised of a fluorescence collecting lens, a multilayer optical interference filter, and an annular a-Si:H PIN photodiode. Separations of multiplex PCR products generated directly from methicillin resistant/sensitive *S. aureus* (MRSA/MSSA) cells and from *E. coli* cells are successfully performed with the integrated detector, demonstrating its ability to perform microfluidic PCR-CE-based genetic analysis.

2. Experimental

2.1. Integrated a-Si:H detector

The integrated a-Si:H detector for microfluidic CE analysis is shown in Figure 1. The detector was fabricated according to previously published procedures (Kamei et al., 2003). Briefly, a 2-mm diameter half-ball lens (BK7), a ZnS/YF_3 multilayer long-pass optical interference filter (E512LP, Chroma Technology) with a 250-mm-diameter drilled pinhole and a plasma deposited annular a-Si:H photodiode were assembled and supported by black anodized aluminum, forming a compact platform for attachment to the microfluidic CE device. The outer diameter of the photodiode was 2.5 mm and the pinhole diameter was 0.4 mm. The photodiode was placed 2.9 mm away from the external surface of the microfluidic CE device and the total thickness of the integrated platform was only 3.6 mm. The microfluidic CE device was optically coupled to the integrated detector platform with index-matching fluid. Incident light from an Ar ion laser (488 nm) was introduced normal to the microfluidic CE device through the photodiode. The annular a-Si:H photodiode and transparent glass substrate allowed vertical laser excitation while avoiding direct incidence of excitation light on the photodiode. This design is difficult to realize using a c-Si photodiode because the c-Si wafer is opaque to visible light. The bottom 100-nm-thick Cr electrode layer of the

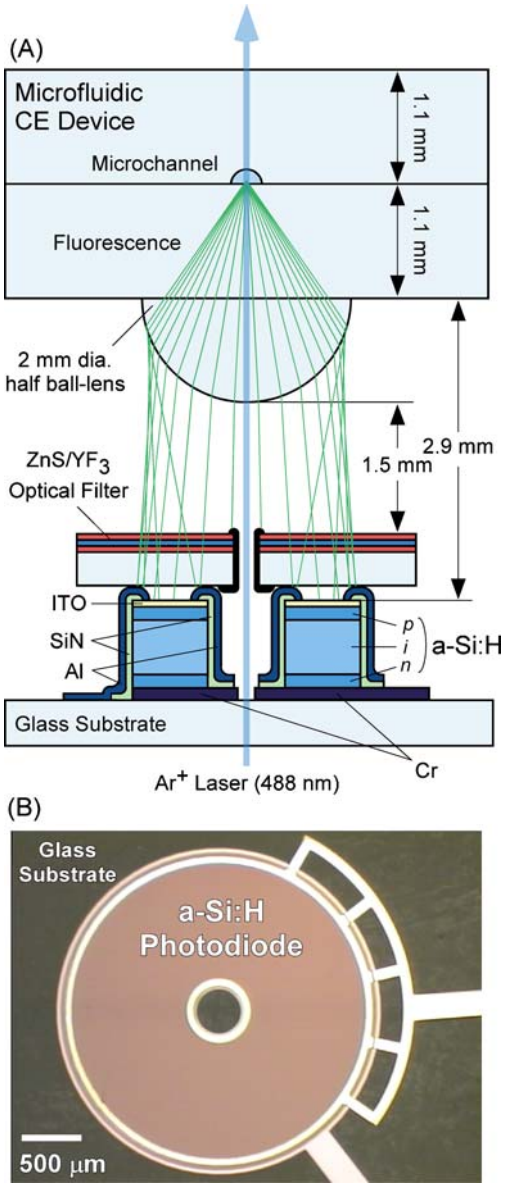

Fig. 1. *(A) Schematic cross-sectional view of the integrated a-Si:H fluorescence detector with a microfluidic electrophoresis device. A ray trace simulation of fluorescence emitted from a microchannel through a 2 mm-dia.-half-ball lens is also shown in green. (B) Optical micrograph of the top view of the annular a-Si:H photodiode.*

a-Si:H photodiode acted as an aperture for the incident laser light. The pinholes in the optical filter and a-Si:H photodiode were coated with flat black paint (blot diameter $\sim$1.2 mm) and a sputtered Al layer, respectively, to prevent laser light scattering from entering the photodiode. A ray trace simulation (ZEMAX, Focus Software) shown in Figure 1 indicated that a 2-mm-diameter BK7 half-ball lens approximately collimates the fluorescence emitted from a microchannel located behind the 1.1-mm-thick borosilicate substrate.

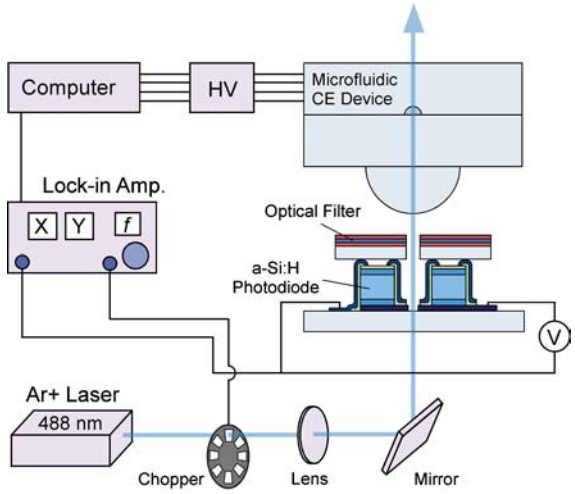

Fig. 2. *A system diagram of the integrated a-Si:H fluorescence detector. The excitation laser beam passes through the chopper, lens, mirror and a-Si:H photodiode and is loosely focused on the microfluidic CE device. The photocurrent under a reverse bias voltage of 1 V was synchronized to the chopped laser light and detected by a lock-in amplifier (LIA). Data acquisition and high voltage (HV) control for separation were accomplished by computer.*

A reverse bias voltage of 1 V was applied to the a-Si:H photodiode to optimize carrier collection efficiency. The photocurrent was synchronized to the chopped laser light at 27 Hz and detected by a lock-in amplifier (LIA) to reduce background. The filtered (300 ms) LIA output was digitized at 50 Hz. Data acquisition and separation control were accomplished using LabView (NI-DAQ 6024E, National Instruments). A diagram of the complete system is shown in Figure 2.

2.2. *Microfluidic CE device fabrication*

The microfluidic CE device was fabricated according to previously published procedures (Simpson et al., 1998). Briefly, borosilicate glass wafers (100 mm diameter, 1.1 mm thick) were patterned using HF wet chemical etching to produce channels 7.8 cm long × 50 μm deep × 120 μm wide for genetic analysis. Access holes were drilled for the sample, waste, cathode, and anode reservoirs and the etched and drilled plate was then thermally bonded to a blank glass plate. Channel arms connecting the injection intersection with the sample, cathode, and waste reservoirs were 0.3, 0.4 and 0.3 cm in length, respectively, for the CE analysis chip.

2.3. *PCR amplification and separation*

The DNA from methicillin-resistant and methicillin-sensitive *Staphylococcus aureus* (MRSA and MSSA) was prepared in the Sensabaugh lab in the School of Public Health at University of California, Berkeley. *E. coli* cells transformed with a pCR 2.1-TOPO plasmid conferring antibiotic resistance to kanamycin (*kan*) were grown overnight at 37°C on LB agar plates. Colonies were picked and suspended in minimal LB broth with kanamycin and grown overnight at 37°C.

The PCR primers used for *S. aureus and E. coli* assay are summarized in Table 1, together with the expected product sizes. The PCR mixture (50 μL) consisted of Qiagen Taq MasterMix kit, 0.2 μM of each primer and 10 ng of either MSSA or MRSA DNA template for the *S. aureus* assay. For the *E. coli* assay the primer concentrations were 0.8 μM and 0.4 μM for K12 and *kan* primers, respectively, and *E. coli* cell concentration was 600 cells/μL. The *S. aureus* PCR was performed in an Eppendorf thermal cycler with a 15 min hotstart polymerase activation at 95°C, followed by a thermal cycling protocol consisting of 42 cycles of 94°C for 30 s, 52°C for 30 s, and 72°C for 60 s. The *E. coli* assay utilized a step-down thermal profile; in the first 5 cycles, the annealing temperature was decreased by 2°C steps from 60 to 52°C while the denaturing and extension temperature were kept constant at 95°C and 72°C, respectively, followed by 34 cycles of 95°C for 30 s, 50°C for 30 s, and 72°C for 60 s. For the separation of the PCR products, hydroxyethylcellulose (HEC, $M_w = 438$ kDa) dissolved in 1× Tris/acetate/EDTA buffer (TAE; 50 mM Tris base, 50 mM acetate, 1 mM EDTA) to 1.4% w/v was used as the sieving matrix. Oxyazole yellow (YO) was diluted to 1 μM

Table 1. *PCR primer sequences and product sizes*

	Forward primer	Reverse primer	Product sizes
S. aureus	*fem A*: 5′-CTTACTTACTGCTGTACCTG-3′	*fem A*: 5′-ATGTCGCTTGTTATGTGC-3′	*fern A*: 219bp
	mecA: 5′-TGGCTATCGTGTCACAATCG-3′	5′-CTGGAACTTGTTGAGCAGAG-3′	*mecA*: 310bp
E. coli	*kan*: 5′-CTGAATGAACTGCAGGACGA-3′	*kan*: 5′-ATACTTTCTCGGCAGGAGCA-3′	*kan*: 172bp
	K12: 5′-ACGCTGCCCGATATAACAAC-3′	K12: 5′-GCAATGGCGTAAAAATTGGT-3′	K12:236bp

concentration in the sieving matrix. The channels were coated with linear polyacrylamide in order to suppress electro-osmotic flow (EOF) and to prevent adsorption of DNA, following a modified Hjertén coating (Hjertén, 1985). The unpurified PCR solution was placed in the sample reservoir and 1× TAE buffer was placed in the waste, cathode, and anode reservoirs to make electrical contact with the platinum electrodes. The PCR products were injected for 30 s from the sample (200 V) to the waste reservoirs (600 V) while applying a pinching potential of 380–400 V at the cathode and anode reservoirs. The separation was then performed with 200 V at the cathode and 2200 V at the anode reservoir while applying 420 V back-biasing potential at the sample and waste reservoirs. A *Hae*III digest of ϕX174 bacteriophage DNA ladder (100 ng/μL) was used to verify the size of the PCR products.

3. Results and Discussions

To characterize the sensitivity of the integrated detector, a fluorescein solution was introduced into a 50-μm deep channel at a constant flow rate of 800 μm/s, which is comparable to the velocity of small DNA fragments under typical CE conditions. Under these conditions, the limit of detection (LOD) at $S/N = 3$ ($N = 2\sigma$) for the integrated a-Si:H detector is 17 nM. The observed LOD is higher than that of a conventional confocal fluorescence detection system (LOD = 10 pM), but it is comparable to the reported LOD for an integrated μAPD detector (Chabinyc et al., 2001). The background signal measured from a buffer-filled channel was around ∼430 pA for a laser power of 0.12 mW. The noise in this high background current primarily restricts the LOD of the integrated detector. When a discrete a-Si:H photodiode was placed in a confocal optical system, the LOD was 680 pM for a laser power of 1 mW, which is 20-fold lower than that of the integrated a-Si:H detector. It is interesting to note that the fluorescence observed with the confocal system is only 2-fold stronger than in the integrated optical system despite a 10-fold difference of excitation power. This difference is principally due to the almost 4-fold larger solid angle of the half ball lens in the integrated system compared to the confocal system (NA = 0.4). The large difference of the LOD in the two systems is primarily due to the superior optical filtering efficacy of the confocal optics.

The background photocurrent of the integrated detector arises predominantly from specular scattering. Possible causes of the specular laser scattering include the non-AR-coated surface of the half ball lens and microfluidic electrophoresis chip, and the side wall of the optical filter pinhole coupled with relatively low optical density (∼3.8) of the long-pass filter at 488 nm. The last point is particularly relevant in comparison with the confocal setup, where a dichroic beam splitter is used to reject the scattered laser light in addition to the band-pass filter. Furthermore, as is inferred from the ray trace simulation in Figure 1, the oblique incidence of the scattered laser light passing from a microchannel through an edge of half ball-lens effectively reduces the optical density of the filter, because the performance of the interference filter is sensitive to the angle of the incident light. Improving the optical filter, metal layer coverage on the sidewall of the filter pinhole, a microlens to produce better light collimation and AR coating of the components, should reduce the background photocurrent and improve the LOD of the a-Si:H detector.

Integrating the detector is a prerequisite for the development of a small, portable genetic analyzer which will find various point-of-care applications ranging from pathogen and infectious disease detection to clinical genetic analysis. Nanoliter-volume microdevices coupling PCR and CE are imperative for specific synthesis of detectable levels of DNA followed by CE analysis to confirm amplicon size. In this study, our goal was to determine whether the sensitivity of the integrated a-Si:H detector is sufficient to directly interrogate microfluidic PCR-CE assays.

S. aureus, a Gram-positive pathogen that is responsible for a wide range of food poisoning, was selected as a model system to demonstrate the feasibility of using the integrated a-Si:H detector for portable pathogen analysis in this study. The methicillin-resistant strain of *S. aureus* is a common source of hospital infections. Therefore, it is necessary not only to detect *S. aureus* but also to identify its strain for clinical treatment and prevention efforts. DNA isolated from methicillin-resistant *S. aureus* (MRSA) or methicillin-sensitive *S. aureus* (MSSA) was introduced into PCR mixtures, leading to a concentration of 200 pg/μL and then amplified. *FemA* is unique to *S. aureus* and thus identifies the DNA as originating from *S.* aureus, while the *mecA* gene confers methicillin resistance (Vannuffel et al., 1998). Figure 3 presents detection of the multiplex PCR products from MRSA and MSSA separated using microchannel CE in comparison with a *Hae*III digest of ϕX174 bacteriophage DNA ladder. As seen in Figure 3, PCR performed using MSSA template DNA, separated on our CE microchannel, and detected using our a-Si:H detector yields only *femA* (219 bp) amplicons while MRSA DNA produces amplicons indicative of both *femA* (219 bp) and *mecA* (310 bp). This result demonstrates genetic discrimination of MRSA from MSSA. Based on calculated peak areas for the bands seen in the *HaeIII* sizing ladder, the LOD ($S/N = 3$) for each fragment is 400–500 pg/μL and the theoretical plates achieved are 50,000, 60,000 and 70,000 for the 194, 234 and 603 bp fragments, respectively. These results demonstrate that integrating the a-Si:H detector with a microfluidic CE device provides the

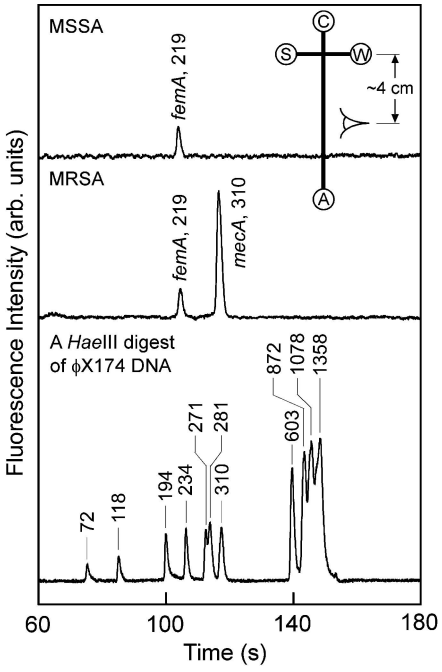

Fig. 3. *Multiplex PCR analysis of MRSA and MSSA with the integrated a-Si:H detector. Top: amplification from MSSA; only the 219 bp peak representing femA gene is observed. Middle: amplification from MRSA; both the 219 bp femA and the 310 bp mecA amplicons are detected. Bottom: a HaeIII digest of ϕX174 bacteriophage DNA (100 ng/μL) ladder for amplicon size reference, run separately on the same device. The inset shows the microfluidic CE device channel geometry, where S, W, C and A stand for sample, waste, cathode and anode reservoirs, respectively. The separation channel was 7.8 cm long, 120 μm wide and 50 μm deep with an effective length 4 cm. Hydroxyethylcellulose (HEC; 1.4 w/v%, $M_w = 438$ kDa) dissolved in 1 × TAE buffer was used as the sieving matrix, and the separation was performed at 250 V/cm. On-column fluorescent labeling was accomplished with the DNA intercalating dye oxyazole yellow (YO, 1 μM).*

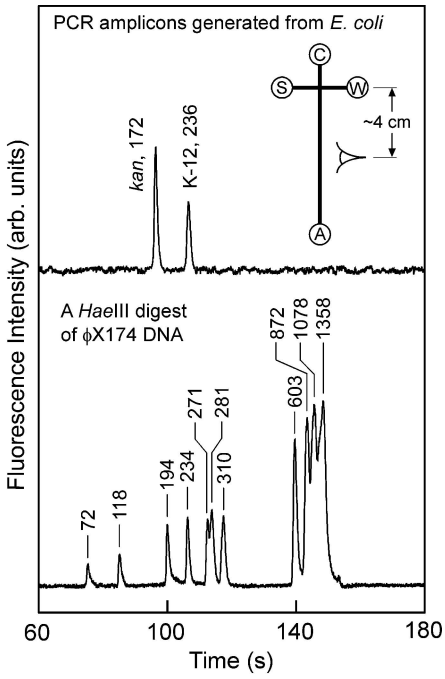

Fig. 4. *Microfluidic separations of multiplex PCR products generated directly from kan resistant K12 E. coli cells and detected with the integrated a-Si:H detector. Upper: amplification from E. coli cells where both the 172 and 236 bp amplicons corresponding kan resistance and the K12 serotype markers are detected. Lower: a HaeIII digest of ϕX174 bacteriophage DNA (100 ng/mL) ladder for amplicon size reference, run separately on the same device. The separation microdevice and conditions are the same as those shown in Figure 3.*

necessary high sensitivity as well as high separation efficiency required for point-of-care genetic detection.

Figure 4 presents the microfluidic separation of multiplex PCR amplicons from kanamycin-resistant *E. coli* cells. *E. coli* cell were introduced into the PCR mastermix at a final concentration of 600 cells/μL. The cells were lysed during the 15 min thermal activation of the polymerase and then amplified. Primers specific to the kanamycin resistance gene and to a K12 serotype-specific gene shown in Table 1 produce 172 and 236 bp amplicons, respectively. Both amplicons were successfully resolved and detected with good signal to noise. The slightly higher intensity of the *kan* amplicon is likely due to the presence of several plasmids in a single transformed *E. coli* cell rather than non-linearities of the PCR amplification. Despite the presence of small ions in the crude PCR solution that lower the electrokinetic injection efficiency of the PCR amplicons and reduce the S/N ratio (Paegel et al., 2002), the integrated a-Si:H detector can detect non-purified PCR amplicons produced from whole cells. This demonstrates the possibility of directly detecting and identifying infectious *E. coli* strains such as O157:H7. Therefore, the integrated detector is sufficiently sensitive for incorporation into current portable microfluidic PCR-CE systems where a nanoliter PCR reactor is directly connected to the separation channel (Lagally et al., 2000, 2004). Since the microfluidic PCR chamber reduces thermal cycling time to <30 min, the combined system should be capable of high speed point-of-analysis pathogen detection and serotyping.

In the future, more complete integration of the fluorescence detection system is possible. We plan to monolithically integrate ZnS/YF_3 filter on the a-Si:H photodiode. From the viewpoint of laser integration, an important aspect of the present device is vertical laser excitation through the detector, enabling a coaxial configuration of laser and detector. When combined with vertical cavity surface emitting laser (VCSEL) diodes, it should be possible to construct a detachable, compact, reusable fluorescence detection unit that integrates VCSEL lasers and detectors for large-scale integrated microfluidic devices.

4. Conclusion

We have developed an integrated a-Si:H fluorescence detection module for microfabricated CE chips where the detection module is reusable. Monolithic integration of an a-Si:H fluorescence detector onto a self-contained glass microfluidic PCR-CE pathogen characterization system is also possible. The direct detection of multiplex PCR amplicons without purification using our integrated fluorescence detection module demonstrates limits of detection for the current microfluidic PCR-CE separation and detection system that are relevant for genetic identification and differentiation of clinically relevant pathogens.

Acknowledgments

We thank Prof. George Sensabaugh for providing the MRSA and MSSA DNA samples. We also acknowledge microfluidic chip fabrication by Stephanie Yeung and a-Si:H photodiode fabrication by Jackson Ho at the Palo Alto Research Center. Microfluidic electrophoresis chip fabrication was carried out at the University of California, Berkeley Microfabrication Laboratory. This research was supported by grants from the National Institutes of Health (HG01399) and from the Director, Office of Science, Office of Biological and Environmental Research of the U.S. Department of Energy under Contract (DE-FG03-91ER61125). T.K. is supported by Industrial Technology Research Grant Program (04A34008) from New Energy and Industrial Technology Development Organization (NEDO) in Japan.

References

M.L. Chabinyc, D.T. Chiu, J.C. McDonald, A.D. Stroock, J.F. Christian, A.M. Karger, and G.M. Whitesides, Anal. Chem. **73**, 4491 (2001).

C.A. Emrich, H.J. Tian, I.L. Medintz, and R.A. Mathies, Anal. Chem. **74**, 5076 (2002).

S. Hjertén, J. Chromatogr. **347**, 191 (1985).

T. Kamei, B.M. Paegel, J.R. Scherer, A.M. Skelley, R.A. Street, and R.A. Mathies, Anal. Chem. **75**, 5300 (2003).

E.T. Lagally, J.R. Scherer, R.G. Blazej, N.M. Toriello, B.A. Diep, M. Ramchandani, G.F. Sensabaugh, L.W. Riley, and R.A. Mathies, Anal. Chem. **76**, 3162 (2004).

E.T. Lagally, P.C. Simpson, and R.A. Mathies, Sens. Actuator B-Chem. **63**, 138 (2000).

M.A. McClain, C.T. Culbertson, S.C. Jacobson, N.L. Allbritton, C.E. Sims, and J.M. Ramsey, Anal. Chem. **75**, 5646 (2003).

B.M. Paegel, C.A. Emrich, G.J. Weyemayer, J.R. Scherer, and R.A. Mathies, Proc. Natl. Acad. Sci. U.S.A. **99**, 574 (2002).

B.M. Paegel, S.H.I. Yeung, and R.A. Mathies, Anal. Chem. **74**, 5092 (2002).

P.C. Simpson, D. Roach, A.T. Woolley, T. Thorsen, R. Johnston, G.F. Sensabaugh, and R.A. Mathies, Proc. Natl. Acad. Sci. U.S.A. **95**, 2256 (1998).

P. Vannuffel, P.F. Laterre, M. Bouyer, J. Gigi, B. Vandercam, M. Reynaert, and J.L. Gala, Journal of Clinical Microbiology **36**, 2366 (1998).

J.R. Webster, M.A. Burns, D.T. Burke, and C.H. Mastrangelo, Anal. Chem. **73**, 1622 (2001).

A.T. Woolley, D. Hadley, P. Landre, A.J. deMello, R.A. Mathies, and M.A. Northrup, Anal. Chem. **68**, 4081 (1996).

A.T. Woolley and R.A. Mathies, Proc. Natl. Acad. Sci. U.S.A. **91**, 11348 (1994).

A.T. Woolley and R.A. Mathies, Anal. Chem. **67**, 3676 (1995).

G.M. Yee, N.I. Maluf, G.T.A. Kovacs, P.A. Hing, and M. Albin, Sensors and Actuators A-Physical **58**, 61 (1997).